

# FTIR and *ab Initio* Studies of Gaseous Nitrosoketene via Pyrolysis of Isonitroso Meldrum's Acid

Hiroshi Matsui\*<sup>†</sup> and Eric J. Zückerman

Department of Chemistry, Purdue University, West Lafayette, Indiana 47907

Nobuya Katagiri and Chikara Kaneko

Pharmaceutical Institute, Tohoku University, Aobayama, Sendai 980-77, Japan

Sihyun Ham and David M. Birney

Department of Chemistry and Biochemistry, Texas Tech University, Lubbock, Texas 79409-1061

Received: August 5, 1996; In Final Form: March 24, 1997<sup>⊗</sup>

Pyrolysis of isonitroso Meldrum's acid is probed to generate gaseous nitrosoketene at temperatures above 80 °C under vacuum in a static system by FTIR and mass spectroscopies. Previously, cyclic nitrones were synthesized from the isonitroso Meldrum's acid in refluxing toluene and ketones. This spectroscopic observation gives a support that cycloaddition of nitrosoketene and ketones gives the cyclic nitrones. Further evidence for the production of nitrosoketene is given by the comparison of vibrational frequencies between experimental results and *ab initio* calculations. At temperatures exceeding 160 °C, nitrosoketene undergoes decarbonylation, forming CO.

## I. Introduction

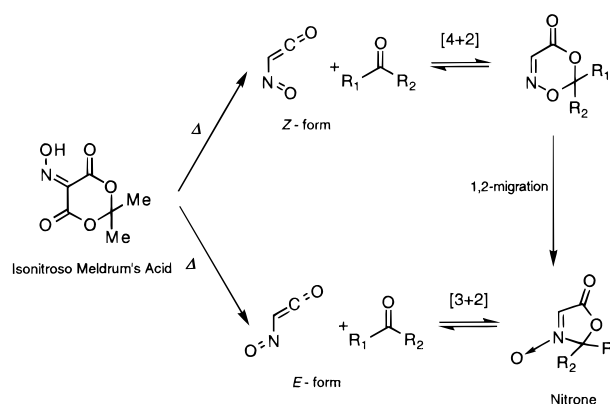
Despite a long history, ketenes continue to be intensively studied. Recently, the kinetic and mechanistic aspects of the thermal decomposition for ketenes have received particular attention, due to their synthetic utility in organic chemistry.<sup>1</sup> For example, the thermal decomposition of ketenes offers a convenient source of carbenes.<sup>2</sup> Catalyzed pyrolysis of ketenes provides polymerization of ketenes, which are of current interest due to their electronic and optical properties.<sup>3</sup>

Nitrosoketene is expected to serve as a useful precursor for the synthesis of many other functional heterocyclic compounds. For example, the cycloaddition of ketones with nitrosoketene generates the cyclic nitrones. This new route to produce nitrones is very useful for the stereoselective synthesis of  $\alpha$ -amino acids having various functional groups.<sup>4,5</sup>

Recently, a synthesis of cyclic nitrones from 5-isonitroso-2,2-dimethyl-1,3-dioxane-4,6-dione (isonitroso Meldrum's acid) with various ketones has been reported.<sup>6,7</sup> Then two possible reaction pathways are considered via nitrosoketene as an intermediate.

In Scheme 1, both of the reaction pathways presume the intermediary of nitrosoketene. RHG/6-31G\* *ab initio* calculations suggest that the direct, pseudopericyclic [3 + 2] cycloaddition of *E*-nitrosoketene to formaldehyde is favored over the indirect [4 + 2] cycloaddition of *Z*-nitrosoketene followed by a possibly ionic 1,2-migration,<sup>8</sup> while the calculated asynchronicity of this transition state, in which C–N bond formation leads that of the C–O, would not predict the observed higher yield of products obtained in the cycloaddition of *p*-methoxyacetophenone as compared to *p*-nitroacetophenone.<sup>7</sup> Despite the fact that several cyclic nitrones have been synthesized via this cycloaddition mechanism, nitrosoketene has not been observed, and there is no experimental evidence concerning the conformation of this reactive intermediate.<sup>6,7</sup>

## SCHEME 1



High-resolution spectroscopic study of intermediates, excited states, and short-lived species always suffers complications due to solvation. To avoid this limitation, gas phase approaches to the detection and characterization of reactive intermediates has been applied for long time.<sup>9</sup> Of course, the study of reaction dynamics and kinetics in the gas phase has been known to have familiar analogies in solution.<sup>10</sup> Accounting for these advantages, we have undertaken a study of the decomposition of isonitroso Meldrum's acid in the gas phase using Fourier transform infrared spectrometry (FTIR) and mass spectrometry. The comparison between experimental absorbances and computed infrared absorbances by *ab initio* calculations shows the presence of nitrosoketene as the intermediate.

## II. Experimental Section

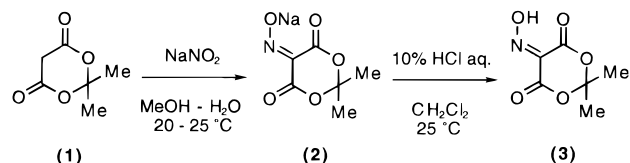
Isonitroso Meldrum's acid is prepared as shown in Scheme 2. Compound **3** was prepared by a modification of the procedure previously reported.<sup>11</sup> A solution of NaNO<sub>2</sub> (4.14 g, 0.06 mol, in 10 mL of water) was added dropwise to a solution of Meldrum's acid (**1**) (7.2 g, 0.05 mol, in 50 mL of methanol) with stirring. This exothermic reaction was cooled

\* Corresponding author.

<sup>†</sup> Present address: Department of Chemistry, Columbia University, New York, NY 10027.

<sup>⊗</sup> Abstract published in *Advance ACS Abstracts*, May 1, 1997.

## SCHEME 2



with a water bath to maintain the temperature at 20–25 °C for 1.5 h, the resulting precipitates were collected by suction (yield was 7.0 g, 71%). Without further purification, the crude product could be used for the next reaction (preparation of compound 3).

Sodium salt (2) (4.9 g, 0.025 mol) was added portionwise to a mixture of 10% HCl (25 mL) and  $\text{CH}_2\text{Cl}_2$  (25 mL) with stirring. The mixture was shaken in a separating funnel. The  $\text{CH}_2\text{Cl}_2$  layer was separated. The aqueous layer was saturated with NaCl and extracted with  $\text{CH}_2\text{Cl}_2$  (15 mL  $\times$  2). The combined  $\text{CH}_2\text{Cl}_2$  solution was dried over anhydrous  $\text{MgSO}_4$ . After evaporation of the solvent, the resulting crystals (3.08 g, 70%) were recrystallized from  $\text{CH}_2\text{Cl}_2$  (20 mL) to give 3 (1.93 g) as pale yellow needles of mp 109–110 °C.

The sample cell consists of a stainless-steel 2.75-in. conflat flange cross and window flanges with 3-mm  $\text{CaF}_2$  flats to allow transmission of the infrared probe radiation. Copper gaskets are used to ensure a vacuum-tight seal between the body of the cell and the flanges. The windows are affixed to flanges by Thermoset DC80 variable flex adhesive, which at a mixture of 2:1 hardener to resin has sufficient flexibility to permit heating to 200 °C.

The cell is heated by an Aerorod stainless-steel tubular heater, wound over the entire surface to provide homogeneous heating. As insulator barriers, a layer of aluminum foil and spun fiberglass tape are wound over the heater. Extra heating is needed around the  $\text{CaF}_2$  windows to avoid adhesion of the sample to the windows. Thus, the window region was preheated to 90 °C with heating tape prior to heating the sample cell. This preheating was not enough to vaporize the sample in the cell, which was confirmed by FTIR measurement. Temperature is controlled by a thermistor (Thermometrics), capable of 0.1 °C precision. The heater and temperature sensor are coupled by a Hart Scientific Model 2100 controller.

The sample ( $6.94 \times 10^{-4}$  mol) in this cell is evacuated to  $10^{-4}$  Torr by a diffusion pump for 12 h to minimize water vapor in the cell through a stainless-steel bellows valve. Products are monitored as a function of temperature, employing a Mattson Polaris FTIR spectrometer with DTGS detector. All spectra are taken with  $1.0 \text{ cm}^{-1}$  resolution.

The mass spectra of the products are recorded by a Finnigan triple stage quadrupole (TSQ) 700 mass spectrometer. The gaseous products in the sample cell are introduced into the source through the GC inlet with a Granville Phillips variable leak valve at sufficient pressure. CI mass spectra are taken with isobutane as a reagent gas. Collisional activation in quadrupole 2 employs 70 eV collision energy, an argon target at a nominal pressure of 3 Torr, and emission current is 300 mA. The spectra are then scanned in quadrupole 3.

## III. Results

FTIR spectra for pyrolyzed species from isonitroso Meldrum's acid are recorded at various temperatures. Figure 1a is the FTIR spectrum taken below 150 °C. Since isonitroso Meldrum's acid has been reported to decompose to acetone and  $\text{CO}_2$  via pyrolysis,<sup>7</sup> we record individual acetone and  $\text{CO}_2$  spectra using the same sample cell (shown in Figure 1b,c) and compare those

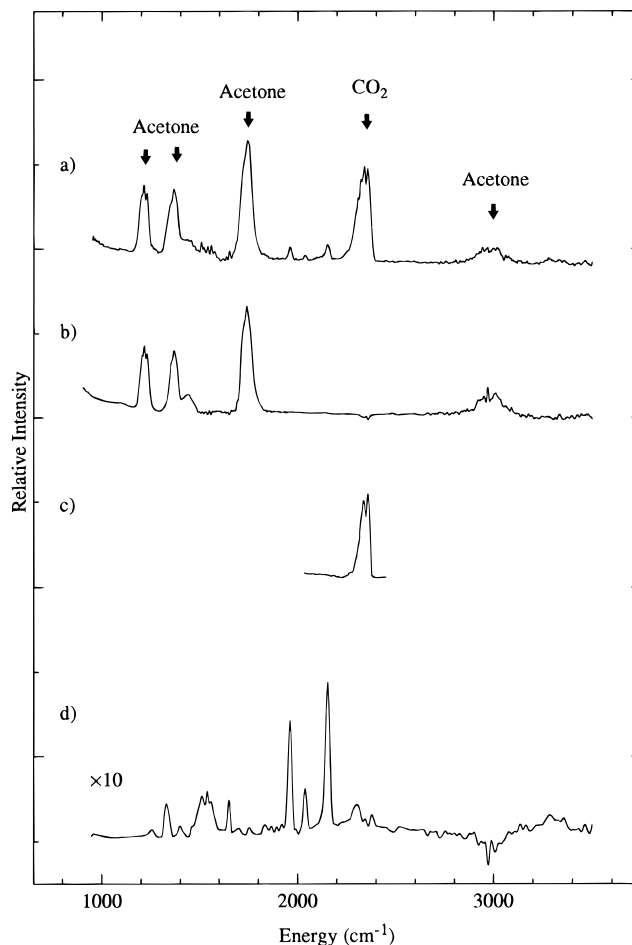


**Figure 1.** (a) FTIR spectrum of the products in the thermal decomposition of isonitroso Meldrum's acid at 150 °C. (b) FTIR spectrum of acetone. (c) FTIR spectrum of  $\text{CO}_2$ . (d) FTIR spectrum of the nitrosoketene with acetone and  $\text{CO}_2$  subtracted.

**TABLE 1: Experimental Absorbances for the Products in the Thermal Decomposition of Isonitroso Meldrum's Acid**

absorbance/ $\text{cm}^{-1}$	qualitative description	absorbance/ $\text{cm}^{-1}$	qualitative description
1219	acetone	1748	acetone
1314	nitrosoketene (C=C stretch)	1965	dimer
1370	acetone	2146	nitrosoketene (C=O stretch)
1438	acetone	2364	$\text{CO}_2$
1531	dimer	2970	acetone
1646	dimer	3300	water

with Figure 1a. This comparison shows that isonitroso Meldrum's acid indeed decomposes to acetone and  $\text{CO}_2$  around 150 °C. Figure 1d shows the FTIR spectrum of the pyrolysis products with acetone and  $\text{CO}_2$  subtracted. The band, as seen at  $2146 \text{ cm}^{-1}$ , is similar to that of ketene,  $2142 \text{ cm}^{-1}$ ,<sup>12</sup> and acetylketene,  $2137 \text{ cm}^{-1}$ ,<sup>13</sup> and therefore this peak is assigned as carbonyl stretch of nitrosoketene. Peaks at 1531, 1646, and  $1965 \text{ cm}^{-1}$  are assigned as the absorbances of a nitrosoketene dimer, and a peak at  $1314 \text{ cm}^{-1}$  is assigned as the C=C stretch mode of the nitrosoketene. Details of these assignments are discussed in the next section. The broad absorbance around  $3300 \text{ cm}^{-1}$  is due to the O–H stretch of water, which evolves from solvent entrapped in the original crystalline sample. This absorbance is independent of temperature variation. Thus, the broad band around  $3300 \text{ cm}^{-1}$  is not including species dissociated from the isonitroso Meldrum's acid. Table 1 contains a

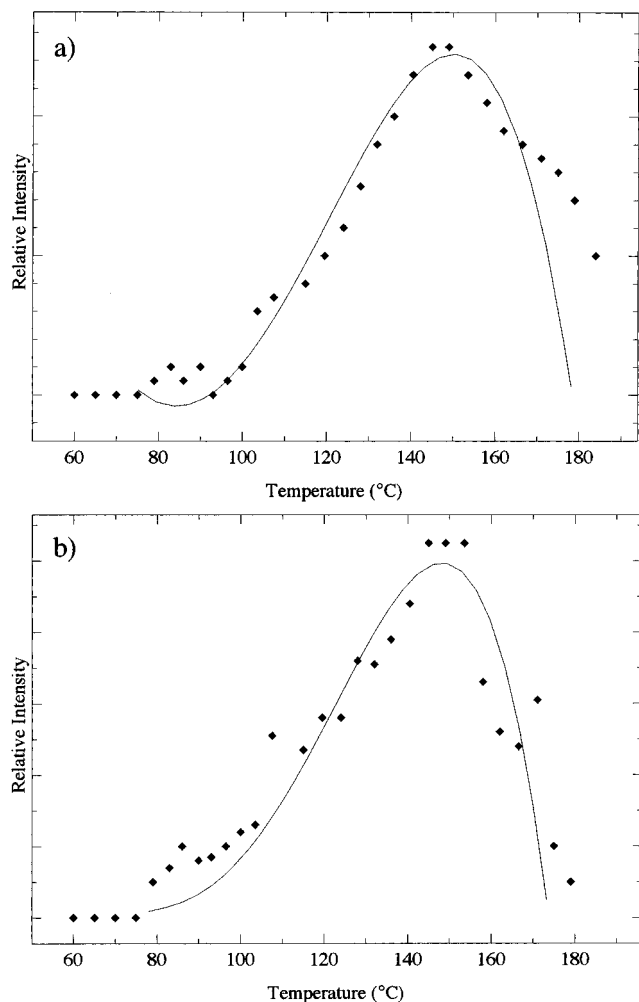


**Figure 2.** Absorbance versus sample cell temperature for (a) C=C stretch of nitrosoketene (at  $1314\text{ cm}^{-1}$ ) and (b) C=O stretch of nitrosoketene (at  $2146\text{ cm}^{-1}$ ).

summary of the relevant FTIR absorption peaks obtained from the experiment.

Mass spectroscopic evidence for the generation of nitrosoketene is obtained by using isobutane CI. At a temperature of  $150\text{ }^{\circ}\text{C}$ , a strong peak at  $m/z = 72$  amu is observed. This peak is considered to be the result of  $\text{H}^+$  addition to nitrosoketene. This observation supports the generation of nitrosoketene following thermal decomposition of isonitroso Meldrum's acid. A weak peak at  $m/z = 143$  amu suggests that a small amount of nitrosoketene dimer is generated even though a fairly low amount of isonitroso Meldrum's acid ( $6.94 \times 10^{-4}$  mol) is vaporized under very low pressure.

#### IV. Discussions

##### Thermolysis Mechanism of Isonitroso Meldrum's Acid.

To confirm the validity of the thermal decomposition of isonitroso Meldrum's acid to nitrosoketene, acetone, and  $\text{CO}_2$ , we plot intensities versus temperatures of the nitrosoketene peaks ( $1314$  and  $2146\text{ cm}^{-1}$ ), acetone peak ( $1219\text{ cm}^{-1}$ ), and  $\text{CO}_2$  peak ( $2330\text{ cm}^{-1}$ ) as shown in Figures 2 and 3. All species are generated at the same temperature, and all increases show the same slope. These plots, thus, indicate that these products are generated simultaneously from isonitroso Meldrum's acid and support the stoichiometry of the thermal decomposition. In Figure 2a,b, the intensity of the  $1314\text{ cm}^{-1}$  absorption shows the same temperature dependence as the C=O stretch of

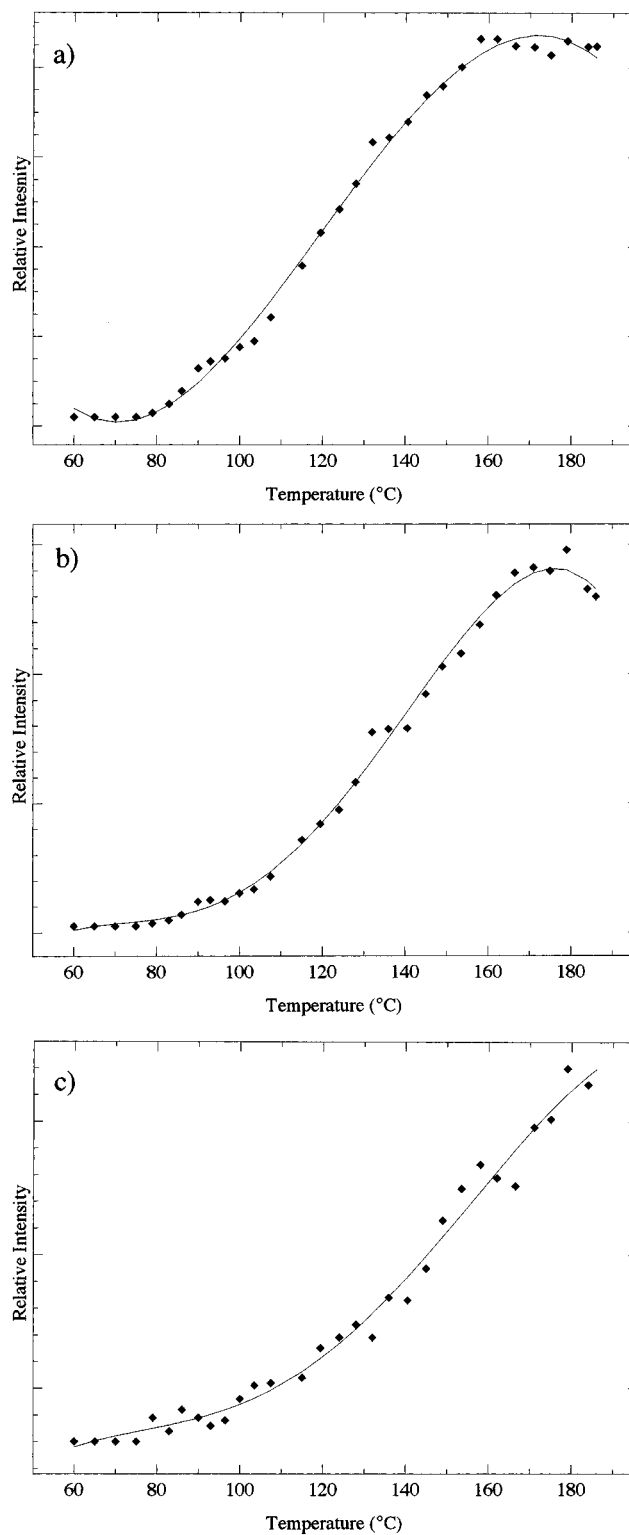


**Figure 3.** Absorbance versus sample cell temperature for (a) acetone (at  $1219\text{ cm}^{-1}$ ), (b)  $\text{CO}_2$  (at  $2364\text{ cm}^{-1}$ ), and (c) dimer (at  $1965\text{ cm}^{-1}$ ).

nitrosoketene peak at  $2146\text{ cm}^{-1}$ , and then this absorption is assigned as the C=C stretch mode of the nitrosoketene.

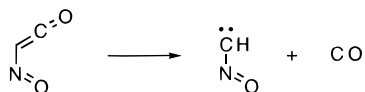
Both acetone (Figure 3a) and  $\text{CO}_2$  (Figure 3b) spectra show increases in their concentration prior to  $150\text{ }^{\circ}\text{C}$  with the same slope, and both plots flatten out after  $150\text{ }^{\circ}\text{C}$ . Thus, the starting species is considered to be completely pyrolyzed at  $150\text{ }^{\circ}\text{C}$  to acetone and  $\text{CO}_2$ .

The absorbance at  $1965\text{ cm}^{-1}$  grows independently with the carbonyl stretch of nitrosoketene and is stable at elevated temperatures (*vide infra*), as shown in Figure 3c. The peaks at

**TABLE 2: Calculated Infrared Absorptivities of Nitrosoketene Dimers and Experimental Infrared Absorptivities of Cyclic Nitron**

	[2 + 2] dimer		[3 + 2] dimer		cyclic nitron
	RHF/6-31G* <sup>a</sup>	int <sup>b</sup>	RHF/6-31G* <sup>a</sup>	int <sup>b</sup>	
C=O			1931	243	
C=O	1930	4	1788	388	1784
C=N	1087	350	1659	329	
N→O	1757	229	1538	4046	1568

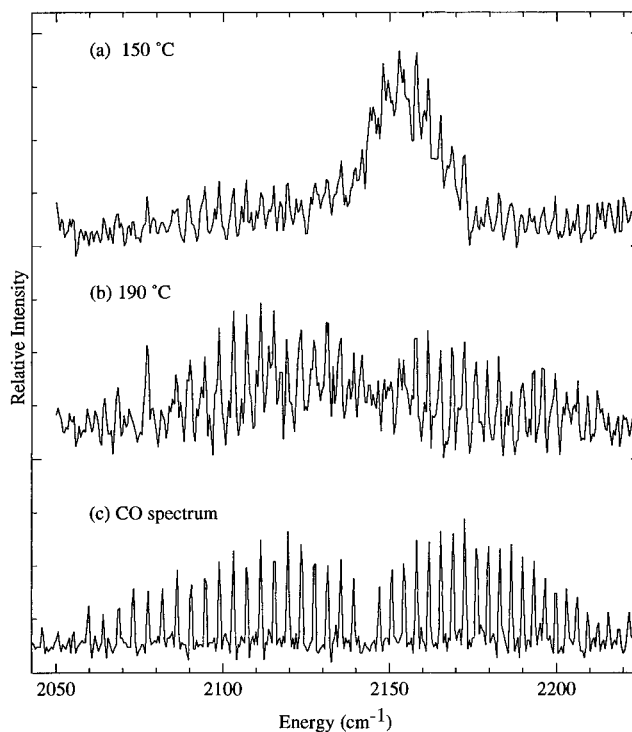
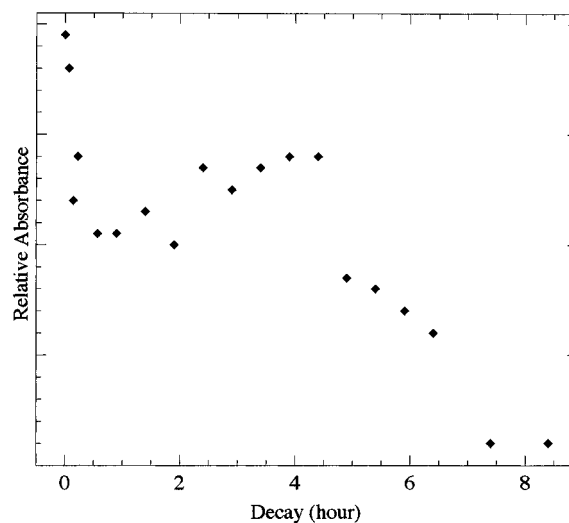
<sup>a</sup> In  $\text{cm}^{-1}$  scaled by 0.8929.<sup>20</sup> <sup>b</sup> In  $\text{km/mol}$ , at the RHF/6-31G\* level. <sup>c</sup> In  $\text{cm}^{-1}$ , ref 6.

**SCHEME 3**

1531 and  $1646\text{ cm}^{-1}$  follow the same trend. Therefore, those peaks are considered to belong to some other species more stable than nitrosoketene. Although dimers of nitrosoketene have not been previously observed, the mass spectral data shows that a dimer is present. Therefore, we have carried out *ab initio* (RHF/6-31G\*) calculations on several potential [2 + 2] and [3 + 2] dimers. Calculated infrared absorptivities of two dimers are represented in Table 2. Due to their size, geometries and absorptivities of the dimers are only calculated at the RHF/6-31G\* level.

The tautomer expected from the [3 + 2] dimerization is calculated (RHF/6-31G\*) to have intense absorptions at  $1538\text{ cm}^{-1}$  (N→O stretch),  $1659\text{ cm}^{-1}$  (C=N stretch), and  $1931\text{ cm}^{-1}$  (C=O stretch). Those calculated frequencies agree well with experimental IR absorptions at 1531, the 1646, and  $1965\text{ cm}^{-1}$ , and therefore those absorptions are assigned to a [3 + 2] dimer of nitrosoketene. While a peak is also calculated at  $1930\text{ cm}^{-1}$  for the *cis*[2 + 2] dimer, it is not as likely to be the origin of the observed  $1965\text{ cm}^{-1}$  band due to very weak intensity by the calculation. No observation of strong absorptions around 1087 and  $1757\text{ cm}^{-1}$ , calculated as C=N stretch and N→O stretch modes for *cis*[2 + 2] dimer, respectively, is also consistent with this assignment. In support of this preliminary assignment, we note that the RHF/6-31G\* level of theory does calculate peaks in the regions observed for C=O and N→O absorptions in similar species, cyclic nitron (2,2-dimethyl-3-oxazolin-5-one 3-oxide), as seen good agreements for these two modes between calculated [3 + 2] dimer and experimental cyclic nitron in Table 2. Although a small peak at  $2039\text{ cm}^{-1}$  has the ketene dimer character, which grows independently of the carbonyl stretch of nitrosoketene and is stable at elevated temperatures, this peak has yet to be identified. Further calculations on various dimers are in progress.

The absorbance for the carbonyl stretch of nitrosoketene decreases at temperatures above  $160\text{ }^\circ\text{C}$ . This is considered to be due to the decarbonylation of nitrosoketene, forming CO (Scheme 3), since a broad absorbance from  $2070$  to  $2200\text{ cm}^{-1}$  is observed at a higher temperature range besides the sharp  $2146\text{ cm}^{-1}$  nitrosoketene peak, as shown in Figure 4b. The spectrum in Figure 4b is matched very well with the CO spectrum shown in Figure 4c. Although we do not observe a strong absorbance of HCNO at  $2190\text{ cm}^{-1}$ ,<sup>14</sup> HCNO and CO are detected by CI mass spectrometry. The absence of the IR absorbance for

**Figure 4.** FTIR spectra in the region from  $2050$  to  $2220\text{ cm}^{-1}$  at (a)  $150$  and (b)  $190\text{ }^\circ\text{C}$ . (c) FTIR spectrum of CO.**Figure 5.** Absorbance versus the decay for nitrosoketene ( $2146\text{ cm}^{-1}$ ) at  $90\text{ }^\circ\text{C}$ .

HCNO may be due to overlap with the broad CO absorbance. No observation of HCN absorbance at  $2097\text{ cm}^{-1}$ <sup>15,16</sup> leads to a conclusion that dissociation of nitrosoketene to HCN and  $\text{CO}_2$  does not occur under our experimental conditions.

To estimate the lifetime of gaseous nitrosoketene, the decay of nitrosoketene at a constant temperature of  $90\text{ }^\circ\text{C}$  is measured and plotted in Figure 5. Under this condition, the gaseous nitrosoketene has a very long lifetime of approximately 4 h. Although the lifetime should be shortened appreciably in solution, this result indicates that nitrosoketene should exist on a time scale large enough to act as the intermediate in the reaction shown in Scheme 1.

Ketenes have been known to be reactive with ketones in solution. Nitrosoketene reacts with acetone, as shown in Scheme 4. The IR spectrum of the product, 2,2-dimethyl-3-oxazolin-5-one 3-oxide, shows two major peaks at 1568 and  $1784\text{ cm}^{-1}$  in ref 7. Because there are no observations of the

## SCHEME 4

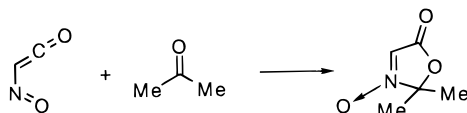


**TABLE 3: Vibrational Frequencies Calculated for Both *E*- and *Z*-Conformations of Nitrosoketene at the MP2/6-31G\* Level**

bands	freq/cm <sup>-1</sup>	scaled freq/cm <sup>-1</sup>		int/km mol <sup>-1</sup>
	MP2/6-31G*	(0.9427)	(0.960)	
<i>Z</i> -Conformation				
C=O	2206	2080	2118	536
N=O	1487	1402		22
C=C	1346	1269		296
<i>E</i> -Conformation				
C=O	2223	2096	2134	655
N=O	1469	1385		85
C=C	1369	1291		60

**TABLE 4: Calculated Relative Energies of *E*- and *Z*-Nitrosoketene in kcal/mol**

	RHF/6-31G*	MP2/6-31G*	MP4(SDQ)/6-31G*+ZPE <sup>a</sup>
<i>Z</i> -nitrosoketene	0.9	1.0	1.1
<i>E</i> -nitrosoketene	0.0	0.0	0.0

<sup>a</sup>Scaled by 0.9646.<sup>20</sup>

1568 and 1784 cm<sup>-1</sup> absorbances in our FTIR spectrum, we consider that the reaction shown in Scheme 4 does not occur in gas phase.

**Ab Initio Calculation and Conformation of Nitrosoketene.** McAllister and Tidwell have calculated a carbonyl stretch of ketene absorption at 2145.0 cm<sup>-1</sup> (scaled by 0.95) for an unspecified conformation of nitrosoketene, at the MP2(FULL)/6-31G\* level.<sup>17</sup> However, in view of our interest in the identification of nitrosoketene and ultimately, its predominant conformation, we optimize the geometries and calculate the vibrational frequencies of both the *E*- and *Z*-conformations at the MP2(FC)/6-31G\* level. These *ab initio* calculations are carried out using Gaussian 92<sup>18</sup> and Gaussian 94.<sup>19</sup> The absorbances calculated at this level are reported in Table 3. The predicted absorbances are scaled using universal factor of 0.9427 as recommended by Pople *et al.*,<sup>20</sup> while the carbonyl stretches of ketenes are scaled using the factor of 0.960 as recommended by Kappe *et al.*<sup>21</sup> Single point energies are calculated at the MP4(SDQ)/6-31G\* level using scaled (0.9626) zero-point energy corrections and are reported in Table 4.

Scaled MP4(SDQ)/6-31G\* level calculations for carbonyl stretches of ketenes are understood to show reasonable agreement with experimental absorbances. For example, the mean absolute error of MP2 carbonyl stretch frequency for acetylketene is 16 cm<sup>-1</sup>, using the scaling factor of 0.9427.<sup>21</sup> Even better agreement between calculated and observed carbonyl stretch frequencies of ketene is obtained using the scaling factor of 0.960 as suggested by Kappe *et al.*<sup>21</sup>

Since we observe only two peaks around 1314 and 2146 cm<sup>-1</sup>, either the *E*- or *Z*- conformer could be generated in the pyrolysis. As shown in Table 3, the differences of calculated frequencies for C=O and C=C stretches between the *E*- and *Z*-conformers are only 16–22 cm<sup>-1</sup>, which are comparable to the mean absolute error of the MP2 carbonyl stretch frequency for acetylketene. Thus, the comparison of vibrational frequencies between the experimental spectrum and this *ab initio* calculations does not allow an accurate assignment of conformation for nitrosoketene.

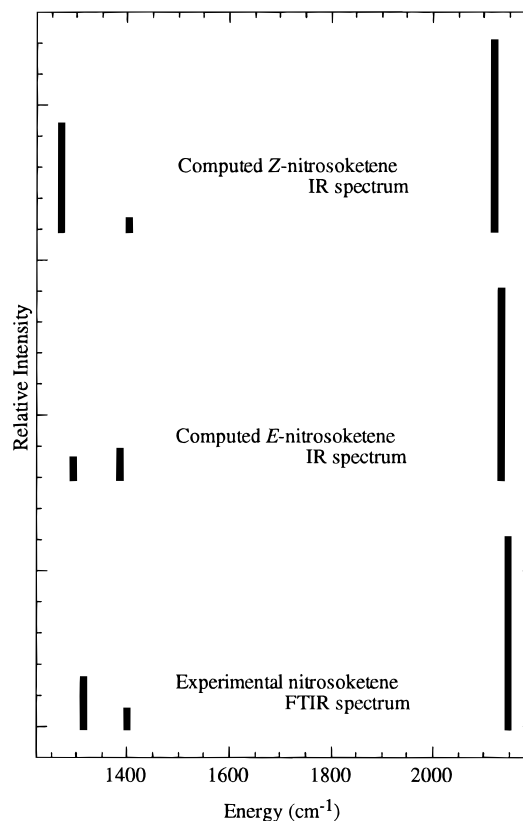


**Figure 6.** Comparison of the computed IR spectra for *Z*- and *E*-nitrosoketene with the experimental FTIR spectrum for nitrosoketene in pyrolysis of isonitroso Meldrum's acid. Relative intensities are normalized to the C=O stretch band.

On the other hand, the calculated IR intensity ratios among the C=O, N=O, and C=C bands are quite different for the *E*- and *Z*- conformers, as shown in Table 3. Although calculated IR intensity for particular vibrational mode should not be compared to an evaluate experimental peak intensity, the overall spectral intensity pattern that is calculated is usually sufficiently accurate to aid in identification of molecular structures.<sup>22</sup> The spectral intensity patterns of the C=C, N=O, and C=O bands in the FTIR experimental spectrum and *ab initio* calculations are summarized in Figure 6. The calculated pattern for the *Z*-conformer agrees better with the experimental spectral pattern, although this agreement is not enough evidence to conclusively determine the conformation of nitrosoketene.

The *E*-conformer is predicted to be more stable than the *Z*-conformer by only 1.1 kcal/mol at the MP4(SDQ)/6-31G\* + ZPE level of theory. Thus this calculation also does not show a strong energetic favor for one conformation of nitrosoketene. Although the conclusive determination of the conformation is not possible from this FTIR spectrum and the *ab initio* calculations, the observed two peaks for nitrosoketene, 1314 and 2146 cm<sup>-1</sup>, are in reasonable agreement with the *ab initio* frequencies for both conformers, which supports that nitrosoketene is the product in pyrolysis of isonitroso Meldrum's acid.

## V. Conclusions

The pyrolysis of isonitroso Meldrum's acid generates nitrosoketene in the temperature-controlled sample cell under vacuum and temperatures above 80 °C. This observation supports the reaction scheme that nitrosoketene serves as the intermediate in the formation of cyclic nitrones from isonitroso Meldrum's acid and ketones. Comparison of vibrational frequencies between experimental results and *ab initio* calcula-

tions also supports the intermediate as nitrosoketene. Although this comparison cannot definitely establish the structure of nitrosoketene due to uncertainties of the experimental and *ab initio* frequencies, the experimental spectral intensity pattern agrees better with the intensity pattern calculated for Z-nitrosoketene. Different methods will be necessary to complete the assessment of conformation for nitrosoketene. We are aware that the group of Wentrup, Visser, Flammang, and Wong is also investigating the formation, reactivity, and spectroscopy of nitrosoketene by FVT/MS/MS, IR spectroscopy, and *ab initio* calculations.<sup>23</sup>

**Acknowledgment.** H.M. gratefully acknowledges a graduate fellowship from the Purdue Research Foundation. This work was supported by the National Science Foundation under Grants No. CHE-8922859 and CHE-9307131 and the Ministry of Education, Science, Sports and Culture, Japan, under Grant 06672230. D.M.B. and S.H. acknowledge support from the Robert A. Welch Foundation. The authors thank Dr. Edward R. Grant for helpful discussions. The authors also thank Dr. Sheng Sheng Yang and Mr. Wenyue Shen for technical assistance with the CI mass spectrometer. We appreciate very helpful comments from all reviewers, which certainly improves the quality of the manuscript.

## References and Notes

- (1) Tidwell, T. T. *Ketenes*; John Wiley & Sons: New York, 1995.
- (2) Allen, W. D.; Schaefer III, H. F. *J. Chem. Phys.* **1986**, *84*, 2212.
- (3) Khemani, K. C.; Wudl, F. *J. Am. Chem. Soc.* **1989**, *111*, 9124.
- (4) DeShong, P.; Lander, S. W., Jr.; Leginus, J. M.; Dicken, C. M. *Advances in Cycloaddition*; Curran, D. P., Ed.; JAI Press: Greenwich, 1988; Vol. 1.
- (5) Confalone, P. N.; Huie, E. M. *Org. React.* **1988**, *36*, 1.
- (6) Katagiri, N.; Kurimoto, A.; Yamada, A.; Sato, H.; Katsuhara, T.; Takagi, K.; Kaneko, C. *J. Chem. Soc., Chem. Commun.* **1994**, 281.
- (7) Katagiri, N.; Sato, H.; Kurimoto, A.; Okada, M.; Yamada, A.; Kaneko, C. *J. Org. Chem.* **1994**, *59*, 8101.
- (8) Ham, S.; Birney, D. M. *Tetrahedron Lett.* **1994**, *35*, 8113.
- (9) Levine, R. D.; Bernstein, R. B. *Molecular Reaction Dynamics*; Oxford University Press: New York, 1974.
- (10) Russell, D. H. *Gas Phase Inorganic Chemistry*; Plenum Press: New York, 1989.
- (11) Briehl, H.; Lukosch, A.; Wentrup, C. *J. Org. Chem.* **1984**, *49*, 2772.
- (12) Moore, C. B.; Pimental, G. C. *J. Chem. Phys.* **1963**, *38*, 2816.
- (13) Clemens, R. J.; Witzeman, J. S. *J. Am. Chem. Soc.* **1989**, *111*, 2186.
- (14) Wentrup, C.; Gerecht, B.; Briehl, H. *Angew. Chem., Int. Ed. Engl.* **1979**, *18*, 467.
- (15) Herzberg, G. *Molecular Spectra and Molecular Structure*; Krieger: New York, 1991; Vol. 3.
- (16) H. C. Allen, J.; Tidwell, E. D.; Plyler, E. K. *J. Chem. Phys.* **1956**, *25*, 302.
- (17) McAllister, M. A.; Tidwell, T. T. *J. Org. Chem.* **1994**, *59*, 4506.
- (18) Frirsch, M. J.; Trucks, G. W.; Head-Gordon, M.; Gill, P. M. W.; Wong, M. W.; Foresman, J. B.; Johnson, B. G.; Schlegel, H. B.; Robb, M. A.; Replogle, E. S.; Gomperts, R.; Andres, J. L.; Raghavachari, K.; Binkley, J. S.; Gonzalez, C.; Martin, R. L.; Fox, D. J.; Defrees, D. J.; Baker, J.; Stewart, J. J. P.; Pople, J. A. *Gaussian 92*; Gaussian, Inc.: Pittsburgh, PA, 1992.
- (19) Frisch, M. J.; Trucks, G. W.; Schlegel, H. B.; Gill, P. M. W.; Johnson, B. G.; Robb, M. A.; Cheeseman, J. R.; Keith, T.; Petersson, G. A.; Montgomery, J. A.; Raghavachari, K.; Al-Laham, M. A.; Zakrzewski, V. G.; Ortiz, J. V.; Foresman, J. B.; Peng, C. Y.; Ayala, P. Y.; Chen, W.; Wong, M. W.; Andres, J. L.; Replogle, E. S.; Gomperts, R.; Martin, R. L.; Fox, D. J.; Binkley, J. S.; Defrees, D. J.; Baker, J.; Stewart, J. J. P.; Head-Gordon, M.; Gonzalez, C.; Pople, J. A. *Gaussian 94*, Gaussian, Inc.: Pittsburgh, PA, 1995.
- (20) Pople, J. A.; Scott, A. P.; Wong, M. W.; Radom, L. *Isr. J. Chem.* **1993**, *345*.
- (21) Kappe, C. O.; Wong, M. W.; Wentrup, C. *J. Org. Chem.* **1995**, *60*, 1686.
- (22) Hess, Jr., B. A.; Schaad, L. J.; Carsky, P.; Zahradnik, R. *Chem. Rev.* **1986**, *86*, 709.
- (23) Visser, P.; Flammang, R.; Wong, M. W.; Wentrup, C. To be published.